

# Southern ocean warming, sea level and hydrological change during the Paleocene-Eocene thermal maximum

A. Sluijs<sup>1</sup>, P. K. Bijl<sup>1</sup>, S. Schouten<sup>2</sup>, U. Röhl<sup>3</sup>, G.-J. Reichert<sup>4</sup>, and H. Brinkhuis<sup>1</sup>

<sup>1</sup>Biomarine Sciences, Institute of Environmental Biology, Utrecht University, Laboratory of Palaeobotany and Palynology, Budapestlaan 4, 3584 CD Utrecht, The Netherlands

<sup>2</sup>Royal Netherlands Institute for Sea Research (NIOZ), Department of Marine Organic Biogeochemistry, P.O. Box 59, 1790 AB, Den Burg, Texel, The Netherlands

<sup>3</sup>Marum – Center for Marine Environmental Sciences, University of Bremen, Leobener Strasse, 28359 Bremen, Germany

<sup>4</sup>Department of Earth Sciences, Utrecht University, Budapestlaan 4, 3584 CD Utrecht, The Netherlands

Received: 9 August 2010 – Published in Clim. Past Discuss.: 8 September 2010

Revised: 20 January 2011 – Accepted: 21 January 2011 – Published: 26 January 2011

**Abstract.** A brief (~150 kyr) period of widespread global average surface warming marks the transition between the Paleocene and Eocene epochs, ~56 million years ago. This so-called “Paleocene-Eocene thermal maximum” (PETM) is associated with the massive injection of <sup>13</sup>C-depleted carbon, reflected in a negative carbon isotope excursion (CIE). Biotic responses include a global abundance peak (acme) of the subtropical dinoflagellate *Apectodinium*. Here we identify the PETM in a marine sedimentary sequence deposited on the East Tasman Plateau at Ocean Drilling Program (ODP) Site 1172 and show, based on the organic paleothermometer TEX<sub>86</sub>, that southwest Pacific sea surface temperatures increased from ~26 °C to ~33 °C during the PETM. Such temperatures before, during and after the PETM are >10 °C warmer than predicted by paleoclimate model simulations for this latitude. In part, this discrepancy may be explained by potential seasonal biases in the TEX<sub>86</sub> proxy in polar oceans. Additionally, the data suggest that not only Arctic, but also Antarctic temperatures may be underestimated in simulations of ancient greenhouse climates by current generation fully coupled climate models. An early influx of abundant *Apectodinium* confirms that environmental change preceded the CIE on a global scale. Organic dinoflagellate cyst assemblages suggest a local decrease in the amount of river run off reaching the core site during the PETM, possibly in concert with eustatic rise. Moreover, the assemblages suggest changes in seasonality of the regional hydrological system and storm activity. Finally, significant variation in

dinoflagellate cyst assemblages during the PETM indicates that southwest Pacific climates varied significantly over time scales of 10<sup>3</sup> – 10<sup>4</sup> years during this event, a finding comparable to similar studies of PETM successions from the New Jersey Shelf.

## 1 Introduction

Gradual widespread warming initiated in the late Paleocene (~59 Ma) and culminated in the Early Eocene Climatic Optimum (EECO; 52–50 Ma) (e.g., Adams et al., 1990; Zachos et al., 2001; Bijl et al., 2009). Superimposed on this long-term warming trend, at least four “hyperthermals” occurred, which represent relatively brief (<200 kyr) intervals characterized by anomalously high temperatures (e.g., Bowen et al., 2006; Sluijs et al., 2007a). The Paleocene-Eocene Thermal Maximum is the most prominent and best-studied hyperthermal and is marked by a negative carbon isotope excursion (CIE) in sedimentary components of 2.5–8‰, depending on analyzed substrate, location and completeness of the section (Kennett and Stott, 1991; Koch et al., 1992; Schouten et al., 2007b). Moreover, massive dissolution of biogenic carbonates occurred in deep ocean basins (e.g., Zachos et al., 2005; Zeebe and Zachos, 2007). The CIE and carbonate dissolution are consistent with geologically rapid, massive injections of <sup>13</sup>C-depleted carbon into the ocean-atmosphere system (Dickens et al., 1997; Panchuk et al., 2008; Zeebe et al., 2009), although the mechanism for such release remains controversial (Dickens et al., 1995; Kurtz et al., 2003; Svensen et al., 2004).



Correspondence to: A. Sluijs  
(A.Sluijs@uu.nl)

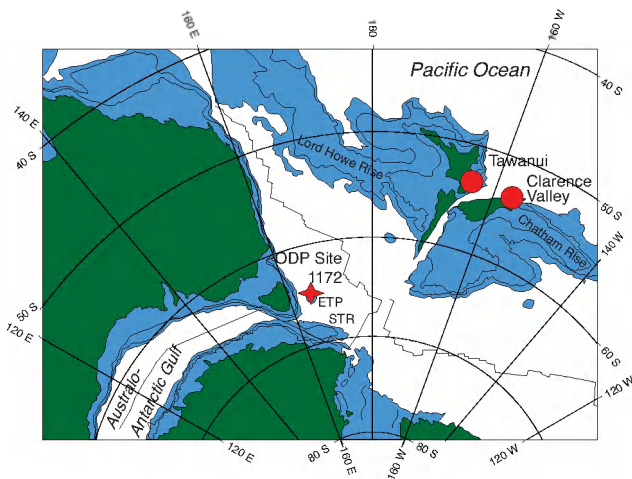


**Fig. 1.** Tectonic reconstruction of the southwest Pacific region for the earliest Eocene, with East Antarctica held fixed, illustrating modern continents (green), areas shallower than 3000 m (blue) and locations of ODP Site 1172 and other sites discussed in the text. ETP = East Tasman Plateau, STR = South Tasman Rise. The figure is modified from Cande and Stock (2004).

Stable oxygen isotope ( $\delta^{18}\text{O}$ ) and Mg/Ca studies on planktonic foraminifera from deep-sea sediments indicate a 5–8 °C surface warming during the PETM (Kennett and Stott, 1991; Thomas et al., 2002; Zachos et al., 2003). Reconstruction of absolute sea surface temperatures (SST) from such sections has been problematic because of post-sedimentary recrystallization of planktonic foraminifera (Schrag et al., 1995; Pearson et al., 2001). Additionally, reduced pH may have dampened foraminifer  $\delta^{18}\text{O}$  excursions, potentially resulting in too low estimates of PETM warming (Uchikawa and Zeebe, 2010). More recently, the application of organic paleothermometers, such as TEX<sub>86</sub> and MBT/CBT in marginal marine sequences provided estimates of absolute temperature evolution across the PETM and other hyperthermals in the Northern Hemisphere (e.g., Sluijs et al., 2006; Zachos et al., 2006; Weijers et al., 2007). This work showed exceptionally high Arctic temperatures during this time interval, suggesting very low meridional temperature gradients (Sluijs et al., 2006). The marginal marine sections used in these studies have also revealed significant increases in river discharge and sediment input (e.g., Crouch et al., 2003; Giusberti et al., 2007; John et al., 2008; Sluijs et al., 2008b; for an overview see Sluijs et al., 2008a), changes in trophic level (e.g., Crouch et al., 2001; Speijer and Wagner, 2002; Gibbs et al., 2006), as well as a globally recorded rise in sea level (Sluijs et al., 2008a). However, temperature and paleoecological data from marginal marine PETM sections from the Southern Hemisphere are rare (Crouch et al., 2001; Crouch and Brinkhuis, 2005), and none are available from the southern high latitudes, hampering thorough evaluation of climatic change in the sub-Antarctic realm.

We have generated geochemical and palynological data through upper Paleocene – lower Eocene sediments recovered during Ocean Drilling Program (ODP) Leg 189 at Site 1172 on the East Tasman Plateau, deposited at ~65° S paleolatitude (Exon et al., 2004) (Fig. 1). Micropaleontological information from the southwest Pacific showed that this site was located within the Antarctic-derived, northward flowing Tasman Current throughout the Paleogene, which is consistent with general circulation model experiments (Huber et al., 2004; Hollis et al., 2009). In an earlier study, based on initial shipboard samples we suggested that the PETM might not have been recovered at this site (Röhl et al., 2004). Here, we identify a condensed PETM section on the basis of a negative CIE in organic matter within magnetochron C24r. We perform TEX<sub>86</sub>, dinoflagellate cyst assemblage analyses and X-ray fluorescence (XRF) core scanning in order to reconstruct paleoenvironmental conditions at southern high latitudes across the PETM.

## 2 Material and methods

### 2.1 Material

Sediments of late Paleocene and early Eocene age at Site 1172, Hole 1172D, consist mainly of organic-rich green and gray clay- and siltstones with low abundance of calcareous and siliceous microfossils, but high abundance of palynomorphs (notably dinocysts but also terrestrial pollen and spores). Glauconite and accessory minerals are recorded in varying abundance (Shipboard Scientific Party, 2001), with the glauconite grains being irregular and angular, which indicates that glauconite was formed in situ (based on thin sections, personal observation, not shown). Lithological and palynological information suggests an overall very shallow marine depositional setting with marked runoff from the nearby shores (Shipboard Scientific Party, 2001; Röhl et al., 2004).

Integrated dinoflagellate cyst and magnetostratigraphic studies identified Chrons C25n, C24r and C24n, with the top of Chron C25n at 618.00 rmbfs and the onset of Chron C24n at 594.2 rmbfs (Fuller and Touchard, 2004; Stickley et al., 2004; Bijl et al., 2009). Average sedimentation rates implied by this age model are 5.7 m/Myr, when assuming a duration of 3.1 Ma for Chron C24r (Westerhold et al., 2007).

### 2.2 Methods

The archive halves of Core 189-1172D-15R were subject to XRF Core Scanning. Subsequently, half-splits of these archive halves were sampled on a resolution of 1 to 2 cm, after which samples were freeze-dried. Splits of samples were then taken for palynology and organic geochemistry. All raw data are provided online in a supplementary data table.

### 2.2.1 X-ray fluorescence (XRF) Core Scanning

We measured the elemental composition of sediments from Cores ODP 189-1172D-15R to -17R at the MARUM, Bremen University, Germany, using the XRF core scanner (Richter et al., 2006; Tjallingii et al., 2007). The XRF core scanner acquires bulk-sediment chemical data from split core surfaces. Although measured elemental intensities are predominantly proportional to concentration, they are also influenced by the energy level of the X-ray source, count time, and physical properties of the sediment (Röhl and Abrams, 2000; Tjallingii et al., 2007). XRF data were collected every cm down-core over a 1 cm<sup>2</sup> area using 30 s count time. We used a generator setting of 20 kV and an X-ray current of 0.15 mA.

### 2.2.2 Palynology

Samples of 1–2 cm stratigraphic thickness were freeze-dried and a known amount of *Lycopodium* spores was added to ~4 g of material. Samples were then treated with 30% HCl and twice with 38% HF for carbonate and silicate removal, respectively. Residues were sieved using a 15- $\mu$ m nylon mesh to remove small particles. To break up clumps of residue, the sample was placed in an ultrasonic bath for a maximum of 5 min, sieved again, and subsequently concentrated into 1 ml of glycerine water, of which 10  $\mu$ l was mounted on microscope slides. Slides were counted for marine (e.g., dinocysts) and terrestrial palynomorphs (e.g., pollen and spores) to a minimum of 200 dinocysts. Marine and terrestrial palynomorph preservation was excellent for all samples. We generally follow dinocyst taxonomy of Fensome and Williams (2004), but follow Sluijs et al. (2009a) for the various spiny peridinioid taxa. Absolute quantitative numbers were counted using the relative abundance of *Lycopodium* spores (cf., Stockmarr, 1972).

### 2.2.3 Organic geochemistry

For stable carbon isotope analyses of total organic carbon ( $\delta^{13}\text{C}_{\text{TOC}}$ ), freeze-dried samples were powdered, treated with 1M HCl to remove carbonate, centrifuged and the supernatant decanted, followed by two rinses with demineralized water and freeze-dried again. Residues were analyzed with a Fison NA 1500 CNS analyzer coupled to a Finnigan Delta Plus isotope ratio mass spectrometer. Analytical precision and accuracy were determined by replicate analyses and by comparison with in-house standards, and were better than 0.1‰ and 0.1‰, respectively.

For biomarker analyses, freeze-dried sediment samples (~3.5 g dry mass) were extracted with dichloromethane (DCM)/methanol (2:1) using accelerated solvent extraction (Dionex ACE). The extracts were separated by Al<sub>2</sub>O<sub>3</sub> column chromatography using hexane/DCM (9:1, v/v) and DCM/methanol (1:1, v/v) to yield the apolar and polar fractions, respectively. The polar fractions were analyzed using

high performance liquid chromatography/atmospheric pressure chemical ionization-mass spectrometry, according to Schouten et al. (2007a). Single ion monitoring was used to quantify the abundance of the Glycerol Dialkyl Glycerol Tetraether (GDGT) lipids. The relative abundance of GDGTs were used to calculate TEX<sub>86</sub> (Schouten et al., 2002). TEX<sub>86</sub> is converted to mean annual SST by means of quasi-global core top calibrations. A new calibration with a logarithmic function was recently published (Kim et al., 2010), which is based on the currently available core-top data and a thorough statistical analyses between GDGTs abundances and SST. An earlier calibration assumes a different logarithmic relation (Liu et al., 2009) that produces particularly different SSTs for high TEX<sub>86</sub> values. We also determined the Branched and Isoprenoid Tetraether (BIT) index. This is a ratio between soil bacteria-derived and marine crenarchaeota-derived membrane lipids, and serves as a proxy for the relative amount of river transported soil organic matter versus marine organic matter (Hopmans et al., 2004).

### 2.2.4 Core depth adjustments

Based on correlations between physical properties data generated on core material and down hole logging, we have slightly changed the meters below sea floor (mbsf) depth of the core sediments in a recent paper (Bijl et al., 2009). We use revised mbsf (rmbsf) for these revised depths throughout. Relative to mbsf, Core 189-1172D-12R was shifted up by 0.36 m, 13R down by 1.87 m, 14R down by 2.84 m, 15R down by 2.4 m, 16R down by 2.57 m and 17R and 18R down by 2.66 m (see also supplementary data table).

## 3 Results

### 3.1 Stratigraphy

Between 611.89 and 611.86 rmbsf, the  $\delta^{13}\text{C}_{\text{TOC}}$  curve shows a ~3‰ negative step from -26 to -29‰, followed by a ~20 cm interval of relatively stable values, and a subsequent exponential recovery that reaches background values between 611.2 and 611.0 rmbsf (Fig. 2). This excursion is located within magnetochron C24r. Average sedimentation rates of 5.7 m/Myrs for this chron (see Material) imply that this excursion occurred ~1 Ma after the termination of Chron C25n (Fuller and Touchard, 2004; Bijl et al., 2009) and ~2 Ma between this CIE and the onset of Chron C24n. The orbitally based age model from Blake Nose (ODP Leg 171B) and Walvis Ridge (ODP Leg 208) also indicates ~1 Ma between the top of Chron C25n and the PETM (Norris and Röhl, 1999), and ~2 Ma between the PETM and the onset of Chron C24n (Westerhold et al., 2007). The onset of Eocene Thermal Maximum 2 occurred ~150 kyrs prior to the reversal of Chron C24r to C24n.3n, which is inconsistent with the location of the recorded CIE. Rather, the overall stratigraphic position of the CIE implies the presence of the PETM in Core

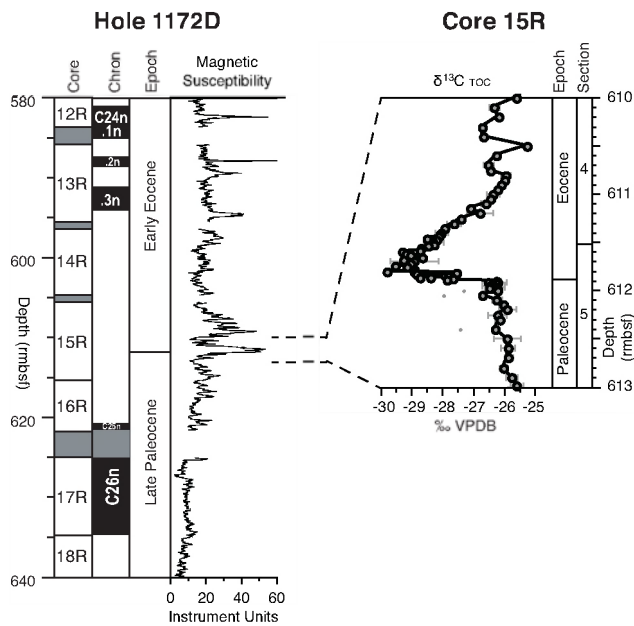


**Fig. 2.** Core recovery and stratigraphic summary of the uppermost Paleocene to earliest Eocene at ODP Site 1172. Note that the core depths are in revised meters below sea floor (rmbfs; see text). Magnetostratigraphic interpretation is from Bijl et al. (2009), which differs from the interpretations published in the first post-cruise papers (Fuller and Touchard, 2004; Röhl et al., 2004) in the assignment of normal polarity intervals to Chrons C25n and C26n. Magnetic susceptibility record represents shipboard data (Shipboard Scientific Party, 2001). Stable carbon isotope ( $\delta^{13}\text{C}$ ) values of total organic carbon (TOC) across the PETM are expressed relative to the Vienna Pee Dee Belemnite standard. Error bars reflect duplicate-based standard deviations and three grey data points are considered outliers because duplicate analyses indicated values consistent with surrounding samples. The figure is modified from Cande and Stock (2004).

1172D-15R. The thickness of the CIE at Site 1172 is 65–90 cm, depending on the definition of its termination (Röhl et al., 2007). Assuming a 170 kyr duration of the CIE (Röhl et al., 2007; Abdul Aziz et al., 2008), this indicates average PETM sedimentation rates of  $\sim 0.4\text{--}0.5\text{ cm/kyr}$ , although sediment accumulation rates were likely highly variable in this pro-deltaic setting.

### 3.2 $\text{TEX}_{86}$ and BIT

Late Paleocene SSTs average  $\sim 26^\circ\text{C}$  ( $1\sigma = 0.9$ ) based on  $\text{TEX}_{86}$ , regardless of the applied calibration (Fig. 2). Concomitantly with the onset of the CIE, SSTs rise to average PETM values of  $\sim 31^\circ\text{C}$  ( $1\sigma = 0.7$ ) following KIM2010, or  $\sim 29^\circ\text{C}$  for LIU2009 with peak values of almost  $33^\circ\text{C}$  and  $31^\circ\text{C}$  for the two calibrations, respectively, at 611.70 rmbfs. The magnitude of PETM warming was thus  $\sim 7^\circ\text{C}$  with KIM2010 and  $4^\circ\text{C}$  with LIU2009. SSTs returned to pre-excursion values during the recovery of the CIE. The warm-

ing and the CIE are preceded by two samples with relatively low temperatures ( $\sim 25^\circ\text{C}$ ).

BIT values are low throughout the analyzed interval, indicating that  $\text{TEX}_{86}$  values are not influenced by soil derived GDGTs (Weijers et al., 2006). The BIT record exhibits some scatter, but values during the PETM ( $0.09 \pm 0.02$ ) are on average somewhat lower than before and after the PETM ( $0.13 \pm 0.03$ ), suggesting increased marine production of isoprenoid GDGTs or a decreased supply of soil organic matter.

### 3.3 Palynology

Palynological assemblages are rich, well preserved and dominated by dinoflagellate cysts (dinocysts). Terrestrial pollen and spores are common to abundant throughout, with relatively high abundances within the PETM (Figs. 2, 3). Stratigraphically important dinocyst taxa include *Apectodinium* spp., *Eocladopyxis peniculatum*, *Deflandrea* spp., *Melittasphaeridium pseudorecurvatum*, *Muratodinium fimbriatum* and the recently described species *Florentinia reichartii* (Sluijs and Brinkhuis, 2009). In particular, the oldest abundant occurrence ( $>40\%$  of the assemblage) of *Apectodinium* in the southwest Pacific Ocean has been calibrated to the PETM (Crouch, 2001). At Site 1172, however, the First Occurrence (FO) of abundant *Apectodinium* is at  $\sim 612.6$  rmbfs,  $\sim 75$  cm below the onset of the CIE (Fig. 3). *Apectodinium* abundances subsequently decrease to  $\sim 2\%$ , followed by a second abundance maximum starting at the onset of the CIE.

Along with *Apectodinium* spp., other quantitatively significant taxa in the assemblage mostly comprise cosmopolitan taxa such as *Senegalinium* spp., *Glaphyrocysta* spp., *Eocladopyxis peniculatum*, *Cordosphaeridium fibrospinosum*, *Thalassiphora* spp., *Kenleyia* spp., *Fibrocysta* spp. (and other members of the *Cordosphaeridium fibrospinosum* complex (sensu, Sluijs and Brinkhuis, 2009), *Diphyes colligerum*, *Paucisphaeridium*, *Deflandrea* (and a few related *Cerodinium*), *Membranospaera* (often referred to as *Elytrocysta* in the Southern Ocean), and *Spiniferites* spp. *Hystri-chosphaeridium truswelliae*, common in certain intervals, was long thought to have been endemic to the Antarctic Realm, but was recently recorded in uppermost Paleocene and PETM sediments on the New Jersey Shelf (Sluijs and Brinkhuis, 2009). In fact, PETM assemblages as a whole are strikingly similar to those reported from the New Jersey Shelf. Only few aspects of the assemblages are typical for the Antarctic Realm (e.g., Wrenn and Beckmann, 1982; Warnaar et al., 2009), including rare *Vozzhennikovia* spp., and temporally abundant *Pyxidinospis* spp.

*Senegalinium* spp. dominate assemblages from the base of the studied section ( $\sim 615$  rmbfs) up to  $\sim 613$  rmbfs, an interval with very stable dinocyst assemblages with common *Pyxidinospis*, *Spiniferites*, and *Deflandrea* spp. Assemblages are slightly richer above  $\sim 613$  rmbfs, with more abundant *Pyxidinospis* spp. and common *H. truswelliae* and *Membranospaera* spp. A peak in *Glaphyrocysta* spp. occurs around



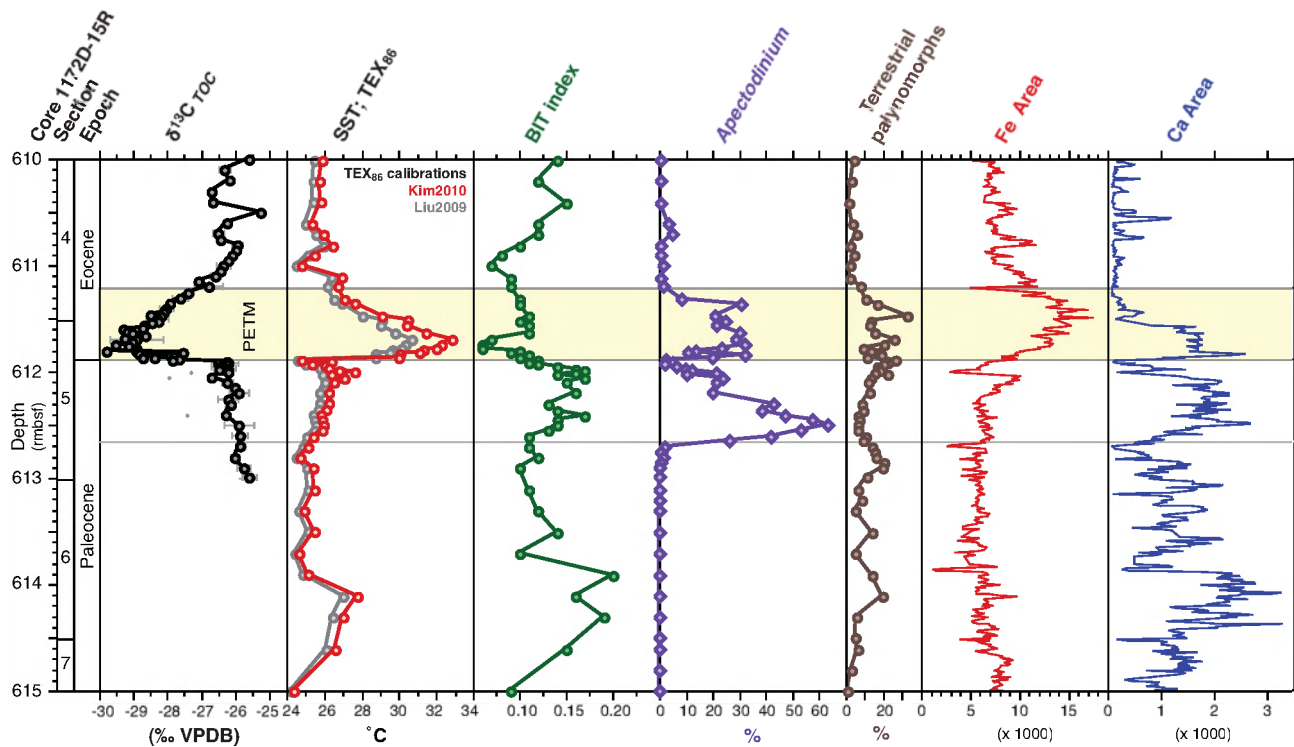


**Fig. 3.** Organic geochemical, palynological and XRF results across the PETM of ODP Site 1172. From left to right: stable carbon isotope ( $\delta^{13}\text{C}$ ) values of total organic carbon (TOC) (see caption at Fig. 2 for details); sea surface temperature (SST) based on  $\text{TEX}_{86}$  following the calibrations KIM2010 (Kim et al., 2010) and LIU2009 (Liu et al., 2009); BIT index; *Apectodinium* percentage of the dinocyst assemblage; abundance of terrestrially derived palynomorphs as a percentage of total pollen and dinocysts; and XRF intensity data for iron and calcium.

613 mbsf, directly followed by the first *Apectodinium* acme. Between 612.2 and 611.9 mbsf, just below the onset of the CIE, successive transient abundances of *Glaphyrocysta*, *Deflandrea*, *Pyxidinospis*, and *Operculodinium* spp., and *C. fibrospinosum* complex occur. A second acme of *Apectodinium* is recorded concomitant with the CIE. Within the CIE, transient abundances of *Glaphyrocysta* spp. and *Eo-cladopyxis peniculatum* occur. After the CIE, *Senegalinium* dominates assemblages again, while *Operculodinium* spp., *H. truswelliae* and *Membranospaera* spp. are common.

### 3.4 XRF

Fe and Ca intensities exhibit a characteristic variability that can be directly attributed to lithology (Fig. 2). The sediments at this site are composed of clay- and siltstones with low abundance of  $\text{CaCO}_3$  (<0.3%), between ~0.5–1% TOC, pyritized diatoms, glauconite, accessory minerals in changing abundance, including varying amounts of quartz (Shipboard Scientific Party, 2001). The dominant lithology is expressed as generally low Ca values in the XRF scans, but the Ca in these sediments is related to carbonate (Röhl et al., 2004). Ca values are higher in the lower part of Core 15R, just three meters below the PETM (Fig. 2). These relatively higher carbonate contents, reflecting higher abundance

of nannofossils, are in line with a shallow marine environment, but compared to the sediments below and above a relatively deeper depositional environment. The Ca intensities in this interval of Core 15R show regular fluctuations: about four cycles below the onset of the PETM, which may also be present in the BIT index, the  $\text{TEX}_{86}$  sea surface temperature data, and reversely in the percentage of terrestrial palynomorphs. Assuming an average sedimentation rate of 5.7 m/Myrs these cycles could represent the low eccentricity frequency of the Milankovitch orbital band (100-kyr cycles). Ca values exhibit peak values during the warming of the PETM, followed by the lowest Ca values in the interval (611.56–610.57 mbsf) (Fig. 2). Ca and Fe are often closely anti-correlated in the pelagic realm, e.g., at ODP Sites 690 and 1263, because abundances of these elements are both forced by carbonate export and preservation (Röhl et al., 2007). Although the Fe and Ca intensities are overall anti-correlated during the PETM at Site 1172 (611.2–611.9 mbsf) their relation is not as strong as in the deep sea. The Fe record exhibits maximum values (broad peak) in the upper part of the CIE, where the Ca values are lower and the terrestrial palynomorphs show maximum values. This indicates that the abundances of these elements are not controlled by carbonate dissolution, as expected for this shallow marine setting (Röhl

et al., 2004), but rather by the sediment supply from land and marine biogeochemical cycling. Indeed, it suggests that the relation of these two main elements Ca and Fe is driven by minor (Milankovitch-driven) variations in clay mineralogy in combination with very low carbonate contents. Ca values stay low above the PETM. In general, for the long-term Site 1172 record including Core 15R, Ca and Fe do not particularly anti-correlate on a larger scale. This is partly caused by the relatively high amount of silica in the sediments in addition to carbonate (Ca) and clay (Fe), which disturbed the perhaps expected anti-correlation of Ca and Fe.

## 4 Discussion

### 4.1 The carbon isotope excursion

The magnitude ( $\sim 3\text{‰}$ ) of the CIE recorded at Site 1172 is similar to or slightly smaller than the 4–5‰ often recorded in  $\delta^{13}\text{C}_{\text{TOC}}$  at other marine sites (Kaiho et al., 1996; Bolle et al., 2000; Crouch et al., 2001; Steurbaut et al., 2003; Sluijs et al., 2006). Since the lowest  $\delta^{13}\text{C}$  values for most carbon isotope records across the PETM are located close to the onset of the event (e.g., Bowen et al., 2001; Thomas et al., 2002; Sluijs et al., 2007a), this could imply that the earliest part of the PETM is not represented in our record. Alternatively, the seemingly damped magnitude of the excursion may be caused by changing sources of organic matter as hypothesized for the small CIE at Tawanui, New Zealand (Crouch et al., 2003), but our palynological analyses do not support major changes in organic matter composition (Figs. 2, 3). Globally, most  $\delta^{13}\text{C}$  curves from the PETM show a rapid drop at the onset, which probably took less than 10 000 years. Subsequently, some bulk carbonate and bulk organic carbon records suggest a slower, sometimes stepwise, continued decline that may span several tens of thousands of years (e.g., Bains et al., 1999; Nicolo et al., 2011). In other records, notably those of single specimen foraminifera, the first negative step is directly followed by  $\sim 80$  kyr of stable carbon isotope values and subsequent recovery that is also recorded in the bulk records, often referred to as the “body” of the CIE (e.g., Thomas et al., 2002; McCarren et al., 2009). Our record clearly shows an interval of stable values of around  $-29\text{‰}$  between  $\sim 611.9\text{--}611.7$  rmbsf, implying that at least part of the stable peak phase is represented in the record. In fact, the magnitude of the CIE in our record is very close to the  $-3$  to  $-3.5\text{‰}$  that is generally assumed to have been the excursion in the global exogenic carbon (Zachos et al., 2007; McCarren et al., 2009). Hence, the record at Site 1172 appears to contain at least a large part of the “body” of the CIE as well as the recovery, allowing comparison to other PETM sites.

## 4.2 Sea surface temperature evolution

### 4.2.1 Magnitude of PETM warming

The range of SST estimates based on  $\text{TEX}_{86}$  is slightly different for the two applied calibrations; LIU2009 gives relatively low temperature estimates and implies a very low sensitivity for  $\text{TEX}_{86}$  values at temperatures  $>30^\circ\text{C}$ . In contrast, KIM2010 implies a higher sensitivity and absolute temperature estimates (Fig. 2). In the New Jersey PETM records for example, the KIM2010 is most consistent with mixed layer planktonic foraminifer stable oxygen isotope ( $\delta^{18}\text{O}$ ) paleothermometry (Kim et al., 2010), also regarding the magnitude of warming. Because the awkwardly low sensitivity of the LIU2009 calibration, and decent multi-proxy intercomparison we prefer the magnitude of warming implied by the KIM2010 calibration in this upper range of  $\text{TEX}_{86}$  values.

A warming of  $\sim 7^\circ\text{C}$  is similar to or slightly less than the only other Southern Ocean estimates from the Weddell Sea (Sites 689 and 690 at Maud Rise), based on the  $\delta^{18}\text{O}$  excursion in the surface dwelling foraminifer *Acarinina* (Thomas et al., 2002; Zachos et al., 2007). The magnitude of the SST rise is also similar to that recorded at marginal marine sites on the New Jersey Shelf based on foraminiferal  $\delta^{18}\text{O}$  and  $\text{TEX}_{86}$  (Zachos et al., 2006; Sluijs et al., 2007b; John et al., 2008). However, the magnitude of warming was smaller in open-ocean and continental settings, and in the Arctic (e.g., Thomas and Shackleton, 1996; Zachos et al., 2003; Tripathi and Elderfield, 2005; Wing et al., 2005; Sluijs et al., 2006; Weijers et al., 2007). This suggests that, while the Arctic warmed with a magnitude comparable to the global average (Sluijs et al., 2006), some marginal marine regions warmed slightly more and some polar amplification may have occurred in the Southern Hemisphere. If so, this amplification may have been caused by three mechanisms. First, the melting of small ice sheets on high mountains in Antarctica may have reduced albedo and thus amplified Antarctic warming. This would be consistent with the reconstructed PETM eustatic rise (Sluijs et al., 2008a). Secondly, an increase in atmospheric heat transport may have occurred. Indeed, increased precipitation in Southern Hemisphere PETM records would suggest more latent heat transport from tropical regions to the Antarctic (Robert and Kennett, 1994; Crouch et al., 2003). However, Arctic sections also exhibit evidence for intensified regional hydrology (Pagani et al., 2006), but no amplification of warming is recorded there (Sluijs et al., 2006). Third, a change in ocean circulation during the PETM may have resulted in regionally enhanced warming in the southwest Pacific and Weddell Sea.

### 4.2.2 Absolute Temperatures

Late Paleocene SSTs average  $\sim 26^\circ\text{C}$  for both the LIU2009 and KIM2010 calibrations (Fig. 2). Average PETM SSTs are  $\sim 31^\circ\text{C}$  following KIM2010 and  $\sim 29^\circ\text{C}$  for LIU2009,

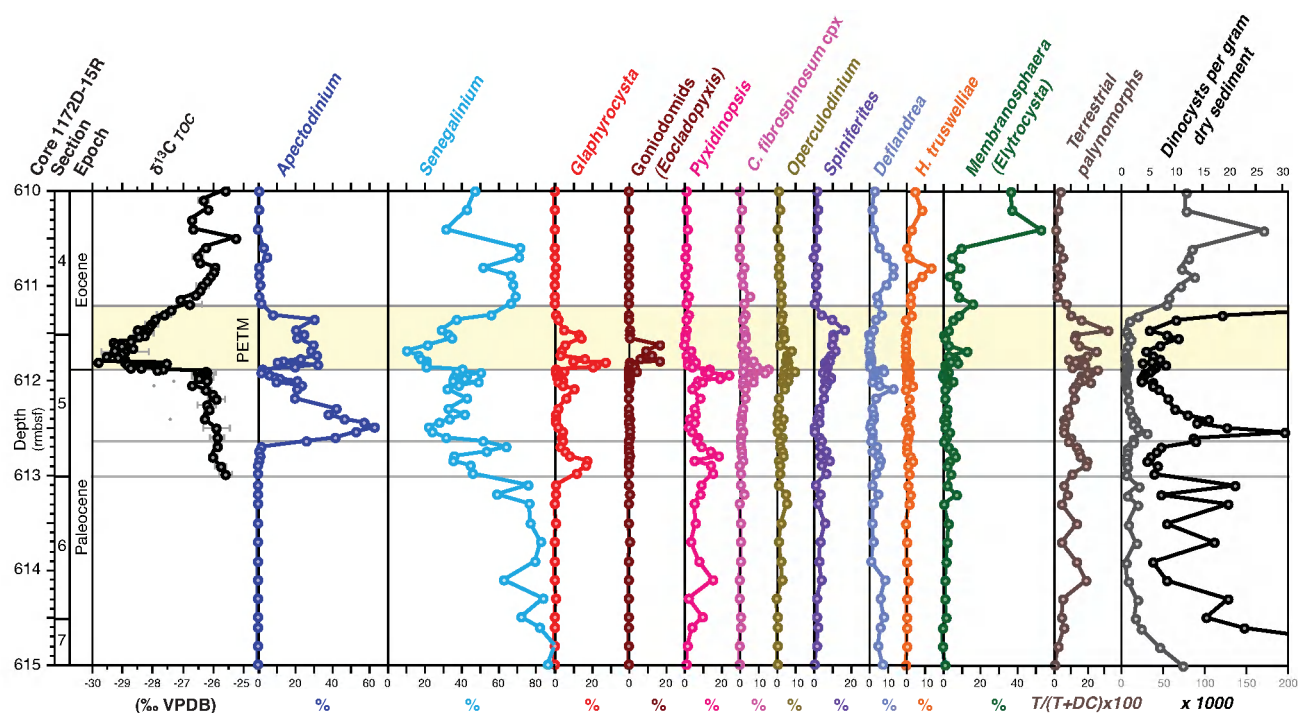


**Fig. 4.** Palynological results across the PETM of Site 1172. Dinocyst abundances are reflected as the percentage of the total dinocyst assemblage and the abundance of terrestrially derived palynomorphs as a percentage of total palynomorph sum. Goniodomids almost exclusively represent *Eocladopyxis peniculatum*. *Membranospaera* is often referred to as *Elytrocyta* in Southern Ocean literature. Grey and black lines in the absolute quantitative dinocyst abundance panel reflect two different scales for illustration purposes.

with peak values of almost 33 °C and 31 °C for the two calibrations, respectively. Because of this calibration difference and as these temperatures are outside the range of modern SSTs, care should be taken in interpreting absolute PETM SST values. Considering the uncertainties of the respective calibrations, TEX<sub>86</sub> indicates that maximum PETM SSTs at Site 1172 were in the range between 29–34 °C.

Although TEX<sub>86</sub> is calibrated to mean annual SST in the modern ocean, like other proxies seasonal and depth biases can occur with the TEX<sub>86</sub> paleothermometer (Huguet et al., 2007; Castaneda et al., 2010). The marine Crenarchaeota (recently renamed Thaumarchaeota; Spang et al., 2010) currently mainly proliferate during winter in both the Arctic and Antarctic oceans (Alonso-Saez et al., 2008; Kalanetra et al., 2009). Likely, this is because most of them are chemolithoautotrophs (Wuchter et al., 2006a), living on ammonia and being not directly depending on light. Also in the present day North Sea they preferentially grow during winter, low light and no competition with algae for ammonia (Wuchter et al., 2006a). Because Crenarchaeota/Thaumarchaeota have low kinetics for ammonia (Martens-Habben et al., 2009), they outcompete bacteria and algae at low ammonia concentrations. These microbiological studies would thus imply that the TEX<sub>86</sub> signal may be even skewed towards winter temperatures. However, the export of membrane lipids to the

sea floor is not necessarily a function of Thaumarchaeotal cell abundance but rather of export through fecal pelleting (Wakeham et al., 2003; Wuchter et al., 2006b). Because the dominant season of export in Paleogene polar oceans was likely summer, we previously suggested that TEX<sub>86</sub> values in such regions might be skewed towards summer temperatures (Sluijs et al., 2006, 2008b; Bijl et al., 2009).

Multi-proxy comparison has indicated good correspondence between TEX<sub>86</sub> and the molecular MBT/CBT proxy for continental air temperature across the PETM in the Arctic (Weijers et al., 2007). Although direct comparison to terrestrial reconstructions in the southwest Pacific is complex, our temperatures are qualitatively consistent with dominant angiosperm pollen in the Site 1172 record. Moreover, records from New Zealand generally exhibit subtropical to tropical floral incursions, including occurrences of the mangrove palm *Nyssa* in the Taranaki, East Coast, and Canterbury Basins (e.g., Crouch and Visscher, 2003; Crouch et al., 2005). In marine sections from New Zealand, TEX<sub>86</sub> agrees with foraminiferal stable oxygen isotope and Mg/Ca ratios in the Eocene (Hollis et al., 2009; Creech et al., 2010). Moreover, TEX<sub>86</sub> and U<sup>K</sup><sub>37</sub> yield similar SST estimates across the Middle Eocene Climatic Optimum (~40 Ma) at Site 1172 (Bijl et al., 2010). However, it should be noted that seasonal biases cannot be excluded in any of these proxies. Oxygen

isotope ratios of reputedly Eocene mollusks from Seymour Island in coastal Antarctica indicate significantly cooler conditions on the Antarctic shelf (Ivany et al., 2008). However, it should be noted that these mollusks are relatively poorly dated and may also be of Middle Eocene age. Nevertheless, if the mollusks are Early Eocene and their  $\delta^{18}\text{O}$  values yield reliable SST estimates, this might imply that  $\text{TEX}_{86}$  is skewed towards summer temperatures. Moreover, temperature estimates for deep sea waters, which at time most likely derived from Antarctic surface waters, are 10–15 °C cooler than our SST estimates (Thomas and Shackleton, 1996; Tripathi and Elderfield, 2005; McCarren et al., 2009). Again, part of this discrepancy can result from seasonal biases. The temperature of deep waters most likely represents winter SST along the Antarctic margin. Collectively, although with the available data it remains impossible to exclude that  $\text{TEX}_{86}$  represents MAT, we consider it likely that the proxy is biased towards summer temperatures in the polar oceans of the Paleogene.

Even if  $\text{TEX}_{86}$  temperatures are skewed towards summer SST estimates, the values are surprisingly high for this latitude, even with the conservative LIU2009 calibration. Pre-PETM SSTs of ~26–27 °C and maximum PETM SSTs of ~30–34 °C are only 3–6 °C cooler than on the New Jersey Shelf at a paleolatitude of ~35–40 °N (Zachos et al., 2006; Sluijs et al., 2007b), and ~8–12 °C warmer than those in the Arctic (Sluijs et al., 2006) depending on the applied calibration. Even if reflect maximum summer temperature estimates, the difference with late Paleocene and early Eocene SSTs 30–35 °C from Tanzania at ~17° S (Pearson et al., 2007) and northern South America at ~10° N (Jaramillo et al., 2010) is extremely small. Originally, the high temperatures in the southern ocean were explained by the supply of warm water through poleward ocean currents (Kennett, 1977; Murphy and Kennett, 1986), but more recent work has indicated that the East Tasman Plateau was more likely influenced by an Antarctic-derived Tasman Current (Huber et al., 2004; Hollis et al., 2009; Bijl et al., 2011). Although the warmest regions have not been sampled yet (Huber, 2008), this supports previous observations (Bijl et al., 2009; Hollis et al., 2009) of a significantly reduced temperature gradient between the southwest Pacific and low latitudes. As indicated for the Northern Hemisphere data (Sluijs et al., 2006, 2007b; Zachos et al., 2006), and then particularly the high winter temperatures (e.g., Sluijs et al., 2009b), the small meridional gradients remain problematic to reconcile with current generation climate models, although recent modeling work has reduced the discrepancy (Abbot et al., 2009; Heinemann et al., 2009).

Interestingly, regardless of the calibration, peak PETM SSTs are similar to those recorded for the EECO at Site 1172 (Bijl et al., 2009). Unless Earth's surface temperatures were not sensitive to changing greenhouse forcing at this high temperature end, this suggests that atmospheric greenhouse gas levels were comparable during the peak of the PETM and

long-term warmth of the EECO. In fact, although regional differences exist, peak PETM temperatures were similar to those during ETM2 (Sluijs et al., 2009b; Stap et al., 2010). If so, one may speculate that the long-term late Paleocene – early Eocene warming and associated carbon isotope trend that culminated in the EECO as well as the superimposed hyperthermals, were caused by carbon injection (Hancock et al., 2007) from the same reservoir. Such a scenario requires a source that slowly added carbon to the global exogenic pool during the long-term trend resulting in the EECO. During the hyperthermals, it must have released carbon catastrophically, perhaps when an orbital (Lourens et al., 2005) threshold was surpassed, followed by partial recharge. One reservoir that may behave like this is the methane hydrate reservoir (Dickens, 2003). Several potential problems exist with methane hydrates as the only source of  $^{13}\text{C}$ -depleted carbon, such as the volume and residence time of this reservoir during the Paleogene. However, a long-term net leakage from hydrates during late Paleocene – early Eocene warming is qualitatively consistent with a concomitant decrease in deep ocean  $\delta^{13}\text{C}$  as observed in benthic foraminiferal calcite (Zachos et al., 2001) and a long-term deepening of the CCD (Hancock et al., 2007).

### 4.3 Leads and lags

The genus *Apectodinium* originated close to the Danian-Selandian boundary (Brinkhuis, 1994; Guasti et al., 2006) but abundant occurrences were restricted to low latitudes until the PETM (Bujak and Brinkhuis, 1998; Iakovleva et al., 2001). On a global scale, *Apectodinium* is an important (often dominant) constituent of the dinoflagellate cyst assemblages described from the PETM (Heilmann-Clausen, 1985; Bujak and Brinkhuis, 1998; Egger et al., 2000; Crouch et al., 2001; Steurbaut et al., 2003; Sluijs et al., 2006; Sluijs et al., 2007a). At Site 1172, however, the lowermost acme starts approximately 70 cm below the CIE.

An influx of abundant *Apectodinium* has also been shown to lead the CIE on the New Jersey Shelf, the Central North Sea and, perhaps, New Zealand (Sluijs et al., 2007b), by approximately 5 kyrs (perhaps slightly longer if sedimentation rates decreased in response to sea level rise; (see, Sluijs et al., 2008a). The early *Apectodinium* acme recorded at Site 1172 can be interpreted in two ways. First, if the uppermost Paleocene record at Site 1172 is relatively expanded, the early acme may actually correlate to the early onset recorded at other sites. Latest Paleocene sedimentation rates of ~10 cm/kyr are required to support this hypothesis, which is significantly higher than the average across this part of the section at Site 1172, but quite common for marginal marine settings. If so, the rise in  $\text{TEX}_{86}$  around 612 rmbfsf might comprise the early warming recorded in New Jersey between the onset of the *Apectodinium* acme and the CIE (Sluijs et al., 2007b), although the latter records do not show a subsequent cooling immediately prior to the onset of the CIE. We cannot



exclude this hypothesis because of the poor constraints on sedimentation rates in the uppermost Paleocene part of the section. Secondly, average sedimentation rates of 5.7 m/Myr suggest that this acme leads the CIE by some 100 kyr. If so, the early *Apectodinium* acme may imply that conditions at Site 1172 locally became similar to low latitude equatorial environments ~100 kyr prior to the CIE, but unrelated to the PETM. This would imply extremely anomalous environmental change on the East Tasman Plateau, associated with the first and mass occurrence of a typical low latitude dinoflagellate in the Southern Ocean, which is not accompanied by significant change in other proxies and, critically, not recorded in nearby sections at lower latitudes in New Zealand (Crouch et al., 2001, 2003; Crouch and Brinkhuis, 2005). Although, this hypothesis seems inconsistent with the strictly low-latitude biogeography of abundant Paleocene *Apectodinium*, we cannot exclude it with the present data.

#### 4.4 Sea level, hydrology and productivity

Low sedimentary Ca values are in line with a shallow marine depositional environment, dominated by siliciclastic input. The Ca record shows a peak during the lower part of the PETM. The persistence of carbonate accumulation in this interval indicates that the CCD resided below the shelf at the East Tasman Plateau during the entire event, consistent with other shelf locations (e.g., Bolle et al., 2000; John et al., 2008).

Representatives of the genus *Senegalinium* dominate dinocyst assemblages for most of the studied interval (Fig. 3). Dinocysts assignable to this genus have been shown to tolerate very low salinities (Brinkhuis et al., 2006). High *Senegalinium* abundances have been associated with salinity stratification on the New Jersey Shelf during the PETM (Sluijs and Brinkhuis, 2009). Moreover, *Senegalinium* likely represents heterotrophic dinoflagellates, thereby thriving in relatively nutrient-rich waters (Sluijs et al., 2005). Accordingly, consistent with lithological information, we interpret high abundances of *Senegalinium* spp. prior to the PETM as to indicate near-shore, relatively high productive shelf settings, with sustained fresh-water runoff from nearby rivers. This interpretation is corroborated by relatively abundant river-transported terrestrial palynomorphs (Fig. 3). Although the low BIT values suggest a relatively low contribution of riverine transported soil derived organic matter, and relative terrestrial palynomorph abundances are not as high as seen in other shelf settings across the PETM (e.g., Crouch et al., 2003; Sluijs et al., 2006) these aspects most likely rather reflect high burial fluxes of marine organic matter and isoprenoid GDGTs compared to terrestrial organic matter.

A decrease in *Senegalinium* abundance at 613.3 mbsf is accompanied by a peak in *Glaphyrocysta* spp., a taxon of which abundant occurrences are often associated with transgressive system tracks and sea level rise (Iakovleva et al., 2001; Pross and Brinkhuis, 2005), suggesting uppermost

Paleocene transgression at Site 1172. Generally increasing abundances of other normal marine taxa, such as *Pyxidinosus* spp., *C. fibrospinosum* cpx., *Spiniferites* spp., and *Operculodinium* spp. support this interpretation. A second peak in *Glaphyrocysta* spp. at the onset of the CIE also suggests renewed sea level rise during the early stages of the PETM, supported by dropping BIT index values and a second drop in *Senegalinium* abundances. This transgression is seen along continental margins on a global scale, including in aspects of dinocyst assemblages in the New Zealand sections (Crouch and Brinkhuis, 2005), and has, hence, shown to represent eustatic rise (Sluijs et al., 2008a).

A record of sea level rise near the Antarctic margin is particularly interesting regarding the potential contributing role of melting Antarctic ice sheets. If an Antarctic ice sheet would have been present in the Paleocene, its self-gravitation should have increased sea level around the continental margin. If the ice sheet melted during the PETM, the loss of gravity should have led to a decrease in sea level during the PETM close to Antarctica, similar to projected for Greenland's margin if the Greenland Ice Sheet would melt (Bamber et al., 2009). Hence, the record of sea level rise during the PETM at Site 1172 might imply that no significant ice sheet was present on Antarctica during the Paleocene.

#### 4.5 Hydrology and sediment supply

Most studied marginal marine sites exhibit a vast increase in sediment supply from the continent during the PETM (Sluijs et al., 2008a), including New Jersey (John et al., 2008), Lomonosov Ridge in the Arctic Ocean (Sluijs et al., 2008b), the North Sea (Steurbaat et al., 2003; Sluijs et al., 2008a), the Bay of Biscay (Schmitz et al., 2001; Pujalte and Schmitz, 2006), the Central Northern Tethys (Giusberti et al., 2007), California (John et al., 2008), and several sections in the southwest Pacific region, notably in New Zealand, such as Tawanui (Crouch et al., 2003) and the Clarence River Valley (Hollis et al., 2005; Nicolo et al., 2011). This is generally interpreted as an increase in terrestrial weathering and resulting supply of siliciclastic material to the shelf by rivers. At Site 1172, no obvious change in average sedimentation rates was recorded during the PETM. This could mean that the strong hydrological response as recorded elsewhere did not take place in the region of the East Tasman Plateau, which is supported by the decrease in fresh-water tolerant dinocysts (Fig. 2). Alternatively, transgression caused sediment condensation at this proximal site. In addition, during the sampling of the core, we did note that the PETM interval is slightly coarser-grained, although, as yet, no data were generated to quantify this. Hence, potentially the sediment-water interface experienced more intense winnowing, hampering the deposition of large amounts of clay.

#### 4.6 Speculations on salinity and storminess

A peak of *Eocladopyxis* spp., a member of the extant family Goniodomidae that mainly inhabits polysaline, lagoonal environments (Wall et al., 1977), occurs within the PETM. Potentially, SSTs were only warm enough for this species to thrive in the Southern Ocean during peak PETM warmth, which may also seasonally have caused regional hypersaline conditions. The ecology of extant Goniodomids provides room for speculations regarding the conditions for the local environment. Abundant representatives of related species in the modern ocean (e.g., the harmful species *Pyrodinium bahamense*) have been related to hypersaline conditions (Reichart et al., 2004). Critically, however, in many regions, seasonal storm activity appears important to resuspend dormant cysts into the water column to hatch and fulfill their life cycle (Villanoy et al., 1996, 2006). In such systems, the subsequent bloom initiates in the wake of the storm when salinities drop due to increased river run off, and when turbulence is minimal (e.g., Dale, 2001; Siringan et al., 2008). Increased river run off and surface ocean stratification might be induced by tropical storms. Hence, storm activity and seasonal river input might have increased in the southwest Pacific region during the PETM, consistent with increased abundances of terrestrial palynomorphs. In any case, a peak in Goniodomids has at Site 1172 only been recorded during the PETM (Fig. 3) and the EECO (Brinkhuis et al., 2003; Sluijs et al., 2003; Bijl, 2007), indicating a very particular environment for this region, likely associated with a change in seasonality of regional hydrology, maximum temperatures and perhaps storm activity.

#### 4.7 Highly variable assemblages within the PETM

The dinocyst record suggests relatively stable conditions through the latest Paleocene and some more variation close to the onset of the CIE and within the PETM, with short-lived abundances of *Glaphyrocysta*, *Eocladopyxis*, *Pyxidinospis*, *Cordosphaeridium fibrospinosum* complex, *Spiniferites*, *Operculodinium*, and *Membranosphaera*. Such intra-PETM variability has also been recorded in continental deposits from Wyoming (Bowen et al., 2004; Wing et al., 2005; Kraus and Riggins, 2007) and on the New Jersey Shelf (Sluijs and Brinkhuis, 2009). Although at the moment the cause of these variations are unknown, they do suggest that climate during the PETM may have been much more variable and dynamic on time scales of  $10^3$ – $10^4$  years, perhaps on a global scale.

### 5 Conclusions

A relatively complete PETM record was identified in sediments recovered from the East Tasman Plateau during ODP Leg 189, deposited at a paleolatitude of  $\sim 65^\circ$  S. Sediments are almost devoid of biogenic calcite but yield rich organic

microfossil assemblages. TEX<sub>86</sub> paleothermometry indicates that SSTs warmed by  $\sim 7^\circ\text{C}$  to maximum values of  $33^\circ\text{C}$  during the PETM, with a magnitude similar to or slightly larger than the global estimate of warming. Such surprisingly warm SSTs for this latitude indicate that meridional temperature gradients were very low across the Paleocene–Eocene transition, even though the reconstructed SSTs may be biased towards summer temperatures. Maximum temperatures were similar to those during the EECO, perhaps implying similar greenhouse gas concentrations. If so, one may speculate that long-term late Paleocene to early Eocene warming, carbon isotope trends and superimposed hyperthermals, were associated with carbon release from the same reservoir, perhaps methane hydrates. The globally recorded acme of the taxon *Apectodinium* leads the CIE at Site 1172, which may represent the same early onset as recorded on the New Jersey Shelf and the North Sea. A decrease in the abundance of the fresh water-tolerant dinoflagellate cyst *Senegalinium* suggests a decrease in the influence of river run off at the core site during the PETM, possibly in concert with sea level rise. However, a unique abundance of the euryhaline taxon *Eocladopyxis* may indicate a change in the seasonality of the regional hydrological system and an increase in storm activity. Finally, significant variations in dinocyst assemblages within the PETM indicate that southwest Pacific climates varied much more significantly over time scales of  $10^3$ – $10^4$  years during the event, than during background late Paleocene – early Eocene times, consistent with records from the New Jersey Shelf and continental North America.

**Supplementary material related to this article is available online at:**

<http://www.clim-past.net/7/47/2011/cp-7-47-2011-supplement.zip>.

**Acknowledgements.** This research used samples and data provided by the Ocean Drilling Program (ODP). Funding for this research was provided by the Netherlands Organisation for Scientific Research to AS (NWO-Veni grant 863.07.001) and SS (NWO-Vici grant), by the Deutsche Forschungsgemeinschaft (DFG) to UR, and by the LPP Foundation to PKB. AS acknowledges the European Research Council under the European Community's Seventh Framework Program for ERC Starting Grant 259627. We thank Dorian Abbot, Jerry Dickens, and Chris Hollis for constructive reviews, Thorsten Kiefer for editorial handling, and Arnold van Dijk, Jan van Tongeren, Natasja Welters (Utrecht University) and Ellen Hopmans and Jort Ossebaar (Royal NIOZ) for technical support.

Edited by: T. Kiefer

## References

- Abbot, D. S., Huber, M., Bousquet, G., and Walker, C. C.: High- $\text{CO}_2$  cloud radiative forcing feedback over both land and ocean in a global climate model, *Geophys. Res. Lett.*, 36, L05702, doi:10.1029/2008gl036703, 2009.
- Abdul Aziz, H., Hilgen, F. J., van Luijk, G. M., Sluijs, A., Kraus, M. J., Pares, J. M., and Gingerich, P. D.: Astronomical climate control on paleosol stacking patterns in the upper Paleocene – lower Eocene Willwood Formation, Bighorn Basin, Wyoming, *Geology*, 36, 531–534, doi:10.1130/G24734A.24731, 2008.
- Adams, C. G., Lee, D. E., and Rosen, B. R.: Conflicting isotopic and biotic evidence for tropical sea-surface temperatures during the Tertiary, *Palaeogeogr. Palaeoclimatol.*, 77, 289–313, 1990.
- Alonso-Saez, L., Sanchez, O., Gasol, J. M., Balague, V., and Pedros-Alio, C.: Winter-to-summer changes in the composition and single-cell activity of near-surface Arctic prokaryotes, *Environ Microbiol.*, 10, 2444–2454, 10.1111/j.1462-2920.2008.01674.x, 2008.
- Bains, S., Corfield, R. M., and Norris, G.: Mechanisms of climate warming at the end of the Paleocene, *Science*, 285, 724–727, 1999.
- Bamber, J. L., Riva, R. E. M., Vermeersen, B. L. A., and LeBrocq, A. M.: Reassessment of the Potential Sea-Level Rise from a Collapse of the West Antarctic Ice Sheet, *Science*, 324, 901–903, doi:10.1126/science.1169335, 2009.
- Bijl, P. K.: Late Paleocene to Early Eocene palaeo-environments in the Southwest Pacific, MSc Thesis, Department of Biology, Utrecht University, Utrecht, 97 pp., 2007.
- Bijl, P. K., Schouten, S., Sluijs, A., Reichert, G.-J., Zachos, J. C., and Brinkhuis, H.: Early Palaeogene temperature evolution of the southwest Pacific Ocean, *Nature*, 461, 776–779, 2009.
- Bijl, P. K., Houben, A. J. P., Schouten, S., Bohaty, S. M., Sluijs, A., Reichert, G.-J., Sinninghe Damsté, J. S., and Brinkhuis, H.: Transient Middle Eocene Atmospheric  $\text{CO}_2$  and Temperature Variations, *Science*, 330, 819–821, doi:10.1126/science.1193654, 2010.
- Bijl, P. K., Pross, J., Warnaar, J., Stickley, C. E., Huber, M., Guerin, R., Houben, A. J. P., Sluijs, A., Visscher, H., and Brinkhuis, H.: Environmental Forcings Of Paleogene Southern Ocean Dinoflagellate Biogeography, *Paleoceanography*, doi:10.1029/2009PA001905, in press, 2011.
- Bolle, M.-P., Pardo, A., Hinrichs, K.-U., Adatte, T., von Salis, K., Burns, S., Keller, G., and Muzylev, N.: The Paleocene-Eocene transition in the marginal northeastern Tethys (Kazakhstan and Uzbekistan), *Int. J. Earth Sci.*, 89, 390–414, 2000.
- Bowen, G. J., Koch, P. L., Gingerich, P. D., Norris, R. D., Bains, S., and Corfield, R. M.: Refined isotope stratigraphy across the continental Paleocene-Eocene boundary on Polecat Bench in the Northern Bighorn Basin, in: *Paleocene-Eocene Stratigraphy and Biotic Change in the Bighorn and Clarks Fork Basins, Wyoming*, edited by: Gingerich, P. D., University of Michigan Papers on Paleontology 33, 73–88, 2001.
- Bowen, G. J., Beerling, D. J., Koch, P. L., Zachos, J. C., and Quatlebaum, T.: A humid climate state during the Palaeocene/Eocene thermal maximum, *Nature*, 432, 495–499, 2004.
- Bowen, G. J., Bralower, T. J., Delaney, M. L., Dickens, G. R., Kelly, D. C., Koch, P. L., Kump, L. R., Meng, J., Sloan, L. C., Thomas, E., Wing, S. L., and Zachos, J. C.: Eocene Hyperthermal Event Offers Insight Into Greenhouse Warming, *EOS, Transactions, American Geophysical Union*, 87, 165, 169, 2006.
- Brinkhuis, H.: Late Eocene to Early Oligocene dinoflagellate cysts from the Priabonian type-area (Northeast Italy): biostratigraphy and palaeoenvironmental interpretation, *Palaeogeography, Palaeoclimatology, Palaeoecology*, 107, 121–163, 1994.
- Brinkhuis, H., Sengers, S., Sluijs, A., Warnaar, J., and Williams, G. L.: Latest Cretaceous to earliest Oligocene, and Quaternary dinoflagellate cysts from ODP Site 1172, East Tasman Plateau., in: *Proceedings Ocean Drilling Program, Scientific Results*, edited by: Exon, N. F., Kennett, J. P., and Malone, M., College Station, Texas, 1–48, 2003.
- Brinkhuis, H., Schouten, S., Collinson, M. E., Sluijs, A., Sinninghe Damsté, J. S., Dickens, G. R., Huber, M., Cronin, T. M., Onodera, J., Takahashi, K., Bujak, J. P., Stein, R., van der Burgh, J., Eldrett, J. S., Harding, I. C., Lotter, A. F., Sangiorgi, F., van Konijnenburg-van Cittert, H., de Leeuw, J. W., Matthiessen, J., Backman, J., Moran, K., and The Expedition 302 Scientists: Episodic fresh surface waters in the Eocene Arctic Ocean, *Nature*, 441, 606–609, 2006.
- Bujak, J. P. and Brinkhuis, H.: Global warming and dinocyst changes across the Paleocene/Eocene Epoch boundary, in: *Late Paleocene – early Eocene climatic and biotic events in the marine and terrestrial records*, edited by: Aubry, M.-P., Lucas, S. G., and Berggren, W. A., Columbia University Press, New York, 277–295, 1998.
- Cande, S. C. and Stock, J. M.: Cenozoic Reconstructions of the Australia-New Zealand-South Pacific Sector of Antarctica, in: *The Cenozoic Southern Ocean: Tectonics, Sedimentation and Climate Change Between Australia and Antarctica. Geophysical Monograph Series 148*, edited by: Exon, N. F., Kennett, J. P., and Malone, M., American Geophysical Union, 5–18, 2004.
- Castaneda, I. S., Schefuss, E., Patzold, J., Sinninghe Damsté, J. S., Weldeab, S., and Schouten, S.: Millennial-scale sea surface temperature changes in the eastern Mediterranean (Nile River Delta region) over the last 27,000 years, *Paleoceanography*, 25, PA1208, doi:10.1029/2009pa001740, 2010.
- Creech, J. B., Baker, J. A., Hollis, C. J., Morgans, H. E. G., and Smith, E. G. C.: Eocene sea temperatures for the mid-latitude southwest Pacific from Mg/Ca ratios in planktonic and benthic foraminifera, *Earth Planet. Sci. Lett.*, 299, 483–495, 2010.
- Crouch, E. M.: Environmental change at the time of the Paleocene-Eocene biotic turnover, *Laboratory of Palaeobotany and Palynology Contribution Series*, 216 pp., 2001.
- Crouch, E. M., Heilmann-Clausen, C., Brinkhuis, H., Morgans, H. E. G., Rogers, K. M., Egger, H., and Schmitz, B.: Global dinoflagellate event associated with the late Paleocene thermal maximum, *Geology*, 29, 315–318, 2001.
- Crouch, E. M., Dickens, G. R., Brinkhuis, H., Aubry, M.-P., Hollis, C. J., Rogers, K. M., and Visscher, H.: The *Apectodinium* acme and terrestrial discharge during the Paleocene-Eocene thermal maximum: new palynological, geochemical and calcareous nannoplankton observations at Tawanui, New Zealand, *Palaeogeogr. Palaeoclimatol.*, 194, 387–403, 2003.
- Crouch, E. M. and Visscher, H.: Terrestrial vegetation record across the initial Eocene thermal maximum at the Tawanui marine section, New Zealand, in: *Causes and Consequences of Globally Warm Climates in the Early Paleogene*, edited by: Wing, S. L., Gingerich, P. D., Schmitz, B., and Thomas, E., Geological Society of America Special Paper 369, Boulder, Colorado, 351–363,

- 2003.
- Crouch, E. M. and Brinkhuis, H.: Environmental change across the Paleocene-Eocene transition from eastern New Zealand: A marine palynological approach, *Mar. Micropaleontol.*, 56, 138–160, 2005.
- Crouch, E. M., Raine, J. I., and Kennedy, E. M.: Vegetation and climate change at the Paleocene-Eocene transition, Geological Society of New Zealand 50th annual conference, Wellington, NZ, 2005, 23.
- Dale, B.: The sedimentary record of dinoflagellate cysts: looking back into the future of phytoplankton blooms, *Sci. Mar.*, 65, 257–272, 2001.
- Dickens, G. R., O'Neil, J. R., Rea, D. K., and Owen, R. M.: Dissociation of oceanic methane hydrate as a cause of the carbon isotope excursion at the end of the Paleocene, *Paleoceanography*, 10, 965–971, 1995.
- Dickens, G. R., Castillo, M. M., and Walker, J. C. G.: A blast of gas in the latest Paleocene: Simulating first-order effects of massive dissociation of oceanic methane hydrate, *Geology*, 25, 259–262, 1997.
- Dickens, G. R.: Rethinking the global carbon cycle with a large, dynamic and microbially mediated gas hydrate capacitor, *Earth Planet. Sci. Lett.*, 213, 169–183, 2003.
- Egger, H., Heilmann-Clausen, C., and Schmitz, B.: The Paleocene-Eocene boundary interval of a Tethyan deep-sea section and its correlation with the North Sea basin, *Bulletin de la Société Géologique de France*, 171, 207–216, 2000.
- Fensome, R. A. and Williams, G. L.: The Lentin and Williams Index of Fossil Dinoflagellates 2004 Edition, American Association of Stratigraphic Palynologists (AASP) Contribution Series 42, 909 pp., 2004.
- Fuller, M. and Touchard, J.: Magnetostratigraphy of Site 1172, Leg 189, in: *The Cenozoic Southern Ocean: Tectonics, Sedimentation, and Climate Change Between Australia and Antarctica*. Geophysical Monograph Series 151, edited by: Exon, N. F., Kennett, J. P., and Malone, M., American Geophysical Union, Washington DC, USA, 2004.
- Gibbs, S. J., Bralower, T. J., Bown, P. R., Zachos, J. C., and Bybell, L. M.: Shelf and open-ocean calcareous phytoplankton assemblages across the Paleocene-Eocene Thermal Maximum: Implications for global productivity gradients, *Geology*, 34, 233–236, 2006.
- Giusberti, L., Rio, D., Agnini, C., Backman, J., Fornaciari, E., Tateo, F., and Oddone, M.: Mode and tempo of the Paleocene-Eocene thermal maximum in an expanded section from the Venetian pre-Alps, *Geol. Soc. Am. Bull.*, 119, 391–412, 2007.
- Guasti, E., Speijer, R. P., Brinkhuis, H., Smit, J., and Steurbaut, E.: Paleoenvironmental change at the Danian-Selandian transition in Tunisia: Foraminifera, organic-walled dinoflagellate cyst and calcareous nannofossil records, *Mar. Micropaleontol.*, 59, 210–229, 2006.
- Hancock, H. J. L., Dickens, G. R., Thomas, E., and Blake, K.: Reappraisal of early Paleogene CCD curves: foraminiferal assemblages and stable carbon isotopes across the carbonate facies of Perth Abyssal Plain, *Int. J. Earth Sci.*, 96, 925–946, 2007.
- Heilmann-Clausen, C.: Dinoflagellate stratigraphy of the Uppermost Danian to Ypresian in the Viborg 1 borehole, Central Jylland, Denmark, *DGU A7*, 1–69, 1985.
- Heinemann, M., Jungclaus, J. H., and Marotzke, J.: Warm Paleocene/Eocene climate as simulated in ECHAM5/MPI-OM, *Clim. Past*, 5, 785–802, doi:10.5194/cp-5-785-2009, 2009.
- Hollis, C. J., Dickens, G. R., Field, B. D., Jones, C. M., and Percy Strong, C.: The Paleocene-Eocene transition at Mead Stream, New Zealand: a southern Pacific record of early Cenozoic global change, *Palaeogeogr. Palaeoclimatol.*, 215, 313–343, 2005.
- Hollis, C. J., Handley, L., Crouch, E. M., Morgans, H. E. G., Baker, J. A., Creech, J., Collins, K. S., Gibbs, S. J., Huber, M., Schouten, S., Zachos, J. C., and Pancost, R. D.: Tropical sea temperatures in the high-latitude South Pacific during the Eocene, *Geology*, 37, 99–102, 2009.
- Hopmans, E. C., Weijers, J. W. H., Schefuß, E., Herfort, L., Sinninghe Damsté, J. S., and Schouten, S.: A novel proxy for terrestrial organic matter in sediments based on branched and isoprenoid tetraether lipids, *Earth Planet. Sci. Lett.*, 224, 107–116, 2004.
- Huber, M., Brinkhuis, H., Stickley, C. E., Döös, K., Sluijs, A., Warnaar, J., Schellenberg, S. A., and Williams, G. L.: Eocene circulation of the Southern Ocean: Was Antarctica kept warm by subtropical waters?, *Paleoceanography*, 19, PA4026, doi:10.1029/2004PA001014, 2004.
- Huber, M.: A Hotter Greenhouse?, *Science*, 321, 353–354, 2008.
- Huguet, C., Schimmelmann, A., Thunell, R., Lourens, L. J., Sinninghe Damsté, J. S., and Schouten, S.: A study of the TEX<sub>86</sub> paleothermometer in the water column and sediments of the Santa Barbara Basin, California, *Paleoceanography*, 22, PA3203, doi:10.1029/2006pa001310, 2007.
- Iakovleva, A. I., Brinkhuis, H., and Cavagnetto, C.: Late Palaeocene-Early Eocene dinoflagellate cysts from the Turgay Strait, Kazakhstan: correlations across ancient seaways, *Palaeogeogr. Palaeoclimatol.*, 172, 243–268, 2001.
- Ivany, L. C., Lohmann, K. C., Hasiuk, F., Blake, D. B., Glass, A., Aronson, R. B., and Moody, R. M.: Eocene climate record of a high southern latitude continental shelf: Seymour Island, Antarctica, *Geol. Soc. Am. Bull.*, 120, 659–678, doi:10.1130/B26269.26261, 2008.
- Jaramillo, C., Ochoa, D., Contreras, L., Pagani, M., Carvajal-Ortiz, H., Pratt, L. M., Krishnan, S., Cardona, A., Romero, M., Quiroz, L., Rodriguez, G., Rueda, M. J., de la Parra, F., Moron, S., Green, W., Bayona, G., Montes, C., Quintero, O., Ramirez, R., Mora, G., Schouten, S., Bermudez, H., Navarrete, R., Parra, F., Alvaran, M., Osorno, J., Crowley, J. L., Valencia, V., and Vervoort, J.: Effects of Rapid Global Warming at the Paleocene-Eocene Boundary on Neotropical Vegetation, *Science*, 330, 957–961, 10.1126/science.1193833, 2010.
- John, C. M., Bohaty, S. M., Zachos, J. C., Sluijs, A., Gibbs, S. J., Brinkhuis, H., and Bralower, T. J.: North American continental margin records of the Paleocene-Eocene thermal maximum: Implications for global carbon and hydrological cycling, *Paleoceanography*, 23, PA2217, doi:10.1029/2007PA001465, 2008.
- Kaiho, K., Arinobu, T., Ishiwatari, R., Morgans, H. E. G., Okada, H., Takeda, N., Tazaki, K., Zhou, G., Kajiura, Y., Matsumoto, R., Hirai, A., Niitsuma, N., and Wada, H.: Latest Paleocene benthic foraminiferal extinction and environmental change at Tawanui, New Zealand, *Paleoceanography*, 11, 447–465, 1996.
- Kalanetra, K. M., Bano, N., and Hollibaugh, J. T.: Ammonia-oxidizing Archaea in the Arctic Ocean and Antarctic coastal waters, *Environ Microbiol.*, 11, 2434–2445, doi:10.1111/j.1462-2920.2009.01974.x, 2009.



- Kennett, J. P.: Cenozoic evolution of Antarctic glaciations, the circum-Antarctic ocean and their impact on global paleoceanography, *J. Geophys. Res.*, 82, 3843–3860, 1977.
- Kennett, J. P. and Stott, L. D.: Abrupt deep-sea warming, palaeoceanographic changes and benthic extinctions at the end of the Palaeocene, *Nature*, 353, 225–229, 1991.
- Kim, J.-H., van der Meer, J., Schouten, S., Helmke, P., Willmott, V., Sangiorgi, F., Koç, N., Hopmans, E. C., and Sinninghe Damsté, J. S.: New indices and calibrations derived from the distribution of crenarchaeal isoprenoid tetraether lipids: Implications for past sea surface temperature reconstructions, *Geochim. Cosmochim. Acta*, 74, 4639–4654, 2010.
- Koch, P. L., Zachos, J. C., and Gingerich, P. D.: Correlation between isotope records in marine and continental carbon reservoirs near the Palaeocene/Eocene boundary, *Nature*, 358, 319–322, 1992.
- Kraus, M. J. and Riggins, S.: Transient drying during the Paleocene-Eocene Thermal Maximum (PETM): Analysis of paleosols in the bighorn basin, Wyoming, *Palaeogeogr. Palaeoclimatol.*, 245, 444–461, 2007.
- Kurtz, A., Kump, L. R., Arthur, M. A., Zachos, J. C., and Paytan, A.: Early Cenozoic decoupling of the global carbon and sulfur cycles, *Paleoceanography*, 18, 1090, doi:10.1029/2003PA000908, 2003.
- Liu, Z., Pagani, M., Zinniker, D., DeConto, R., Huber, M., Brinkhuis, H., Shah, S. R., Leckie, R. M., and Pearson, A.: Global Cooling During the Eocene-Oligocene Climate Transition, *Science*, 323, 1187–1190, doi:10.1126/science.1166368, 2009.
- Lourens, L. J., Sluijs, A., Kroon, D., Zachos, J. C., Thomas, E., Röhl, U., Bowles, J., and Raffi, I.: Astronomical pacing of late Palaeocene to early Eocene global warming events, *Nature*, 435, 1083–1087, 2005.
- Martens-Habben, W., Berube, P. M., Urakawa, H., de la Torre, J. R., and Stahl, D. A.: Ammonia oxidation kinetics determine niche separation of nitrifying Archaea and Bacteria, *Nature*, 461, 976–U234, doi:10.1038/nature08465, 2009.
- McCarren, H., Thomas, E., Hasegawa, T., Röhl, U., and Zachos, J. C.: Depth dependency of the Paleocene-Eocene carbon isotope excursion: Paired benthic and terrestrial biomarker records (Ocean Drilling Program Leg 208, Walvis Ridge), *Geochem. Geophys. Geosyst.*, 9, Q10008, doi:10.1029/2008GC002116, 2009.
- Murphy, M. G. and Kennett, J. P.: Development of latitudinal thermal gradients during the Oligocene: Oxygen isotope evidence from the southwest Pacific., in: Initial Reports of the Deep Sea Drilling Project 90, Washington, US govt. printing office, 1347–1360, 1986.
- Nicolo, M. J., Dickens, G. R., and Hollis, C. J.: South Pacific intermediate water oxygen depletion at the onset of the Paleocene-Eocene Thermal Maximum as depicted in New Zealand margin sections, *Paleoceanography*, in press, 2011.
- Pagani, M., Pedentchouk, N., Huber, M., Sluijs, A., Schouten, S., Brinkhuis, H., Sinninghe Damsté, J. S., Dickens, G. R., and The Expedition 302 Scientists: Arctic hydrology during global warming at the Palaeocene-Eocene thermal maximum, *Nature*, 442, 671–675, 2006.
- Panchuk, K., Ridgwell, A., and Kump, L. R.: Sedimentary response to Paleocene-Eocene Thermal Maximum carbon release: A model-data comparison, *Geology*, 36, 315–318, 2008.
- Pearson, P. N., Ditchfield, P. W., Singano, J., Harcourt-Brown, K. G., Nicholas, C. J., Olsson, R. K., Shackleton, N. J., and Hall, M. A.: Warm tropical sea surface temperatures in the Late Cretaceous and Eocene epochs, *Nature*, 413, 481–487, 2001.
- Pearson, P. N., van Dongen, B. E., Nicholas, C. J., Pancost, R. D., Schouten, S., Singano, J. M., and Wade, B. S.: Stable warm tropical climate through the Eocene Epoch, *Geology*, 35, 211–214, 2007.
- Pross, J. and Brinkhuis, H.: Organic-walled dinoflagellate cysts as paleoenvironmental indicators in the Paleogene; a synopsis of concepts, *Paläontologische Zeitschrift*, 79, 53–59, 2005.
- Pujalte, V. and Schmitz, B.: Abrupt climatic and sea level changes across the Paleocene-Eocene boundary, as recorded in an ancient coastal plain setting (Pyrenees, Spain), *Climate and Biota of the Early Paleogene*, Bilbao, Spain, 2006.
- Reichert, G.-J., Brinkhuis, H., Huiskamp, F., and Zachariasse, W. J.: Hyperstratification following glacial overturning events in the northern Arabian Sea, *Paleoceanography*, 19, PA2013, doi:10.1029/2003PA000900, 2004.
- Richter, T. O., Van der Gast, S., Koster, R., Vaars, A., Gieles, R., De Stigter, H. C., De Haas, H., and Van Weering, T. C. E.: The Avaatech XRF Core Scanner: technical description and applications to NE Atlantic sediments, in: *New Techniques in Sediments Core Analysis*, edited by: Rothwell, R. G., Geological Society London, Special Publication, London, 39–51, 2006.
- Robert, C. and Kennett, J. P.: Antarctic subtropical humid episode at the Paleocene-Eocene boundary: clay mineral evidence, *Geology*, 22, 211–214, 1994.
- Röhl, U. and Abrams, L. J.: High-resolution, downhole and non-destructive core measurements from Sites 999 and 1001 in the Caribbean Sea: application to the Late Paleocene Thermal Maximum, in: *Proceedings of the Ocean Drilling Program (ODP), Scientific Results 165*, Ocean Drilling Program, College Station, TX, 191–203, 2000.
- Röhl, U., Brinkhuis, H., Sluijs, A., and Fuller, M.: On the search for the Paleocene/Eocene Boundary in the Southern Ocean: Exploring ODP Leg 189 Holes 1171D and 1172D, Tasman Sea, in: *The Cenozoic Southern Ocean: Tectonics, Sedimentation, and Climate Change Between Australia and Antarctica*, Geophysical Monograph Series 151, edited by: Exxon, N. F., Malone, M., and Kennett, J. P., 113–125, 2004.
- Röhl, U., Westerhold, T., Bralower, T. J., and Zachos, J. C.: On the duration of the Paleocene – Eocene thermal maximum (PETM), *Geochem., Geophys., Geosyst.*, 8, Q12002, doi:10.1029/2007GC001784, 2007.
- Schmitz, B., Pujalte, V., and Nunez-Betelu, K.: Climate and sea-level perturbations during the Initial Eocene Thermal Maximum: evidence from siliciclastic units in the Basque Basin (Ermua, Zumaia and Trabakua Pass), northern Spain, *Palaeogeography, Palaeoclimatology, Palaeoecology*, 165, 299–320, 2001.
- Schouten, S., Hopmans, E. C., Schefuß, E., and Sinninghe Damsté, J. S.: Distributional variations in marine crenarchaeotal membrane lipids: a new tool for reconstructing ancient sea water temperatures?, *Earth Planet. Sci. Lett.*, 204, 265–274, 2002.
- Schouten, S., Hugué, C., Hopmans, E. C., Kienhuis, M. V. M., and Sinninghe Damsté, J. S.: Analytical Methodology for TEX<sub>86</sub> Paleothermometry by High-Performance Liquid Chromatography/Atmospheric Pressure Chemical Ionization-Mass Spectrom-

- etry, *Anal. Chem.*, 79, 2940–2944, 2007a.
- Schouten, S., Woltering, M., Rijpstra, W. I. C., Sluijs, A., Brinkhuis, H., and Sinninghe Damsté, J. S.: The Paleocene-Eocene carbon isotope excursion in higher plant organic matter: Differential fractionation of angiosperms and conifers in the Arctic, *Earth Planet. Sci. Lett.*, 258, 581–592, 2007b.
- Schrag, D. P., dePaolo, D. J., and Richter, F. M.: Reconstructing past sea surface temperatures: Correcting for diagenesis of bulk marine carbonate, *Geochemica et Cosmochemica Acta*, 59, 2265–2278, 1995.
- Shipboard Scientific Party, X.: Site 1172, in: *Proceedings of the Ocean Drilling Program, Initial Reports*, 189, edited by: Exon, N. F., Kennett, J. P., and Malone, M., Ocean Drilling Program, College Station, TX, 1–149; doi:10.2973/odp.proc.ir.2189.2107.2001, 2001.
- Siringan, F. P., Azanza, R. V., Macalalad, N. J. H., Zamora, P. B., and Sta. Maria, M. Y. Y.: Temporal changes in the cyst densities of *Pyrodinium bahamense* var. *compressum* and other dinoflagellates in Manila Bay, Philippines, *Harmful Algae*, 7, 523–531, 2008.
- Sluijs, A., Brinkhuis, H., Stickley, C. E., Warnaar, J., Williams, G. L., and Fuller, M.: Dinoflagellate cysts from the Eocene/Oligocene transition in the Southern Ocean; results from ODP Leg 189, in: *Proceedings Ocean Drilling Program, Scientific Results 189*, edited by: Exon, N. F., Kennett, J. P., and Malone, M. J., College Station, Texas, 1–42, 2003.
- Sluijs, A., Pross, J., and Brinkhuis, H.: From greenhouse to ice-house; organic-walled dinoflagellate cysts as paleoenvironmental indicators in the Paleogene, *Earth-Sci. Rev.*, 68, 281–315, 2005.
- Sluijs, A., Schouten, S., Pagani, M., Woltering, M., Brinkhuis, H., Sinninghe Damsté, J. S., Dickens, G. R., Huber, M., Reichart, G.-J., Stein, R., Matthiessen, J., Lourens, L. J., Pedentchouk, N., Backman, J., Moran, K., and The Expedition 302 Scientists: Subtropical Arctic Ocean temperatures during the Palaeocene/Eocene thermal maximum, *Nature*, 441, 610–613, 2006.
- Sluijs, A., Bowen, G. J., Brinkhuis, H., Lourens, L. J., and Thomas, E.: The Palaeocene-Eocene thermal maximum super greenhouse: biotic and geochemical signatures, age models and mechanisms of global change, in: *Deep time perspectives on Climate Change: Marrying the Signal from Computer Models and Biological Proxies*, edited by: Williams, M., Haywood, A. M., Gregory, F. J., and Schmidt, D. N., The Micropalaeontological Society, Special Publications. The Geological Society, London, London, 323–347, 2007a.
- Sluijs, A., Brinkhuis, H., Schouten, S., Bohaty, S. M., John, C. M., Zachos, J. C., Reichart, G.-J., Sinninghe Damsté, J. S., Crouch, E. M., and Dickens, G. R.: Environmental precursors to light carbon input at the Paleocene/Eocene boundary, *Nature*, 450, 1218–1221, 2007b.
- Sluijs, A., Brinkhuis, H., Crouch, E. M., John, C. M., Handley, L., Munsterman, D., Bohaty, S. M., Zachos, J. C., Reichart, G.-J., Schouten, S., Pancost, R. D., Sinninghe Damsté, J. S., Welters, N. L. D., Lotter, A. F., and Dickens, G. R.: Eustatic variations during the Paleocene-Eocene greenhouse world, *Paleoceanography*, 23, PA4216, doi:10.1029/2008PA001615, 2008a.
- Sluijs, A., Röhl, U., Schouten, S., Brumsack, H.-J., Sangiorgi, F., Sinninghe Damsté, J. S., and Brinkhuis, H.: Arctic late Paleocene–early Eocene paleoenvironments with special emphasis on the Paleocene-Eocene thermal maximum (Lomonosov Ridge, Integrated Ocean Drilling Program Expedition 302), *Paleoceanography*, 23, PA1S11, doi:10.1029/2007PA001495, 2008b.
- Sluijs, A. and Brinkhuis, H.: A dynamic climate state during the Paleocene-Eocene Thermal Maximum: inferences from dinoflagellate cyst assemblages on the New Jersey Shelf, *Biogeosciences*, 6, 1755–1781, 2009, <http://www.biogeosciences.net/6/1755/2009/>.
- Sluijs, A., Brinkhuis, H., Williams, G. L., and Fensome, R. A.: Taxonomic revision of some Cretaceous-Cenozoic spiny organic-walled, peridinioid dinoflagellate cysts, *Rev. Palaeobot. Palynol.*, 154, 34–53 doi:10.1016/j.revpalbo.2008.1011.1006, 2009a.
- Sluijs, A., Schouten, S., Donders, T. H., Schoon, P. L., Röhl, U., Reichart, G. J., Sangiorgi, F., Kim, J.-H., Sinninghe Damsté, J. S., and Brinkhuis, H.: Warm and Wet Conditions in the Arctic Region during Eocene Thermal Maximum 2, *Nature Geoscience*, 2, 777–780, 2009b.
- Spang, A., Hatzenpichler, R., Brochier-Armanet, C., Rattei, T., Tischler, P., Spieck, E., Streit, W., Stahl, D. A., Wagner, M., and Schleper, C.: Distinct gene set in two different lineages of ammonia-oxidizing archaea supports the phylum Thaumarchaeota, *Trends in Microbiology*, 18, 331–340, 2010.
- Speijer, R. P. and Wagner, T.: Sea-level changes and black shales associated with the late Paleocene thermal maximum: Organic-geochemical and micropaleontologic evidence from the southern Tethyan margin (Egypt-Israel), *Geological Society of America Special Paper*, 356, 533–549, 2002.
- Stap, L., Lourens, L. J., Thomas, E., Sluijs, A., Bohaty, S. M., and Zachos, J. C.: High-resolution deep-sea carbon and oxygen isotope records of Eocene Thermal Maximum 2 and H2, *Geology*, 38, 607–610, 2010.
- Sturbaut, E., Magioncalda, R., Dupuis, C., Van Simaey, S., Roche, E., and Roche, M.: Palynology, paleoenvironments, and organic carbon isotope evolution in lagoonal Paleocene-Eocene boundary settings in North Belgium, in: *Causes and consequences of Globally Warm Climates in the Early Paleogene*, Geological Society of America Special Paper 369, edited by: Wing, S. L., Gingerich, P., Schmitz, B., and Thomas, E., Geological Society of America, Boulder, Colorado, 291–317, 2003.
- Stickley, C. E., Brinkhuis, H., McGonigal, K., Chaproniere, G., Fuller, M., Kelly, D. C., Nürnberg, D., Pfuhl, H. A., Schellenberg, S. A., Schoenfeld, J., Suzuki, N., Touchard, Y., Wei, W., Williams, G. L., Lara, J., and Stant, S. A.: Late Cretaceous-Quaternary biomagnetostratigraphy of ODP Sites 1168, 1170, 1171, and 1172, Tasmanian Gateway, in: *Proceedings of the Ocean Drilling Program, Scientific Results*, 189, edited by: Exon, N. F., Kennett, J. P., and Malone, M. J., College Station, TX, 1–57, 2004.
- Stockmarr, J.: Tablets with spores used in absolute pollen analysis, *Pollen et Spores*, 13, 615–621, 1972.
- Svensen, H., Planke, S., Malthes-Sørensen, A., Jamtveit, B., Myklebust, R., Eidem, T. R., and Rey, S. S.: Release of methane from a volcanic basin as a mechanism for initial Eocene global warming, *Nature*, 429, 542–545, 2004.
- Thomas, D. J., Zachos, J. C., Bralower, T. J., Thomas, E., and Bohaty, S.: Warming the fuel for the fire: Evidence for the thermal dissociation of methane hydrate during the Paleocene-Eocene thermal maximum, *Geology*, 30, 1067–1070, 2002.
- Thomas, E. and Shackleton, N. J.: The Palaeocene-Eocene benthic

- foraminiferal extinction and stable isotope anomalies., in: Correlation of the Early Paleogene in Northwestern Europe, Geological Society London Special Publication, 101, edited by: Knox, R. W. O. B., Corfield, R. M., and Dunay, R. E., Geological Society of London, London, United Kingdom, 401–441, 1996.
- Tjallingii, R., Röhl, U., Kölling, M., and Bickert, T.: Influence of the water content on X-ray fluorescence core scanning measurements in soft marine sediments, *Geochemistry, Geophysics, Geosystems*, Technical Brief, 8, Q02004, doi:10.1029/20006GC001393, 2007.
- Tripathi, A. and Elderfield, H.: Deep-Sea Temperature and Circulation Changes at the Paleocene-Eocene Thermal Maximum, *Science*, 308, 1894–1898, 2005.
- Uchikawa, J. and Zeebe, R. E.: Examining possible effects of sea-water pH decline on foraminiferal stable isotopes during the Paleocene-Eocene Thermal Maximum, *Paleoceanography*, 25, PA2216, doi:10.1029/2009PA001864, 2010.
- Villanoy, C., Corralet, R. A., Jacinto, G. S., Cuaserna, N., and Crisostomo, R.: Towards the development of a cyst-based model for *Pyrodinium* red tides in Manila Bay, in: Harmful Toxic Algal Blooms, edited by: Yasumoto, T., Oshima, Y., and Fukuyo, Y., IOC of UNESCO, Paris, 189–192, 1996.
- Villanoy, C. L., Azanza, R. V., Altemerano, A., and Casil, A. L.: Attempts to model the bloom dynamics of *Pyrodinium*, a tropical toxic dinoflagellate, *Harmful Algae*, 5, 156–183, 2006.
- Wakeham, S. G., Lewis, C. M., Hopmans, E. C., Schouten, S., and Sinninghe Damsté, J. S.: Archaea mediate anaerobic oxidation of methane in deep euxinic waters of the Black Sea, *Geochim. Cosmochim. Ac.*, 67, 1359–1374, 2003.
- Wall, D., Dale, B., Lohmann, G. P., and Smith, W. K.: The environmental and climatic distribution of dinoflagellate cysts in modern marine sediments from regions in the North and South Atlantic Oceans and adjacent seas, *Marine Micropaleontology*, 2, 121–200, 1977.
- Warnaar, J., Bijl, P. K., Huber, M., Sloan, L., Brinkhuis, H., Röhl, U., Sriver, R., and Visscher, H.: Orbitally forced climate changes in the Tasman sector during the Middle Eocene, *Palaeogeogr. Palaeoclimatol.*, 280, 361–370, 2009.
- Weijers, J. W. H., Schouten, S., Spaargaren, O. C., and Sinninghe Damsté, J. S.: Occurrence and distribution of tetraether membrane lipids in soils: Implications for the use of the TEX<sub>86</sub> proxy and the BIT index, *Org. Geochem.*, 37, 1680–1693, 2006.
- Weijers, J. W. H., Schouten, S., Sluijs, A., Brinkhuis, H., and Sinninghe Damsté, J. S.: Warm arctic continents during the Palaeocene-Eocene thermal maximum, *Earth Planet. Sci. Lett.*, 261, 230–238, 2007.
- Westerhold, T., Röhl, U., Laskar, J., Raffi, I., Bowles, J., Lourens, L. J., and Zachos, J. C.: On the duration of Magnetochrons C24r and C25n, and the timing of early Eocene global warming events: Implications from the ODP Leg 208 Walvis Ridge depth transect, *Paleoceanography*, 22, PA2201, doi:10.1029/2006PA001322, 2007.
- Wing, S. L., Harrington, G. J., Smith, F. A., Bloch, J. I., Boyer, D. M., and Freeman, K. H.: Transient Floral Change and Rapid Global Warming at the Paleocene-Eocene Boundary, *Science*, 310, 993–996, doi:10.1126/science.1116913, 2005.
- Wrenn, J. H. and Beckmann, S. W.: Maceral, total organic carbon, and palynological analyses of Ross Ice Shelf Project site J9 cores, *Science*, 216, 187–189, 1982.
- Wuchter, C., Abbas, B., Coolen, M. J. L., Herfort, L., van Bleijswijk, J., Timmers, P., Strous, M., Teira, E., Herndl, G. J., Middeburg, J. J., Schouten, S., and Damste, J. S. S.: Archaeal nitrification in the ocean, *Proceedings of the National Academy of Sciences of the United States of America*, 103, 12317–12322, doi:10.1073/pnas.0600756103, 2006a.
- Wuchter, C., Schouten, S., Wakeham, S. G., and Sinninghe Damsté, J. S.: Archaeal tetraether membrane lipid fluxes in the northeastern Pacific and the Arabian Sea: Implications for TEX<sub>86</sub> paleothermometry, *Paleoceanography*, 21, PA4208, doi:10.1029/2006PA001279, 2006b.
- Zachos, J., Pagani, M., Sloan, L., Thomas, E., and Billups, K.: Trends, Rhythms, and Aberrations in Global Climate 65 Ma to Present, *Science*, 292, 686–693, doi:10.1126/science.1059412, 2001.
- Zachos, J. C., Wara, M. W., Bohaty, S., Delaney, M. L., Petrizzo, M. R., Brill, A., Bralower, T. J., and Premoli Silva, I.: A transient rise in tropical sea surface temperature during the Paleocene-Eocene thermal maximum, *Science*, 302, 1551–1554, 2003.
- Zachos, J. C., Röhl, U., Schellenberg, S. A., Sluijs, A., Hodell, D. A., Kelly, D. C., Thomas, E., Nicolo, M., Raffi, I., Lourens, L. J., McCarren, H., and Kroon, D.: Rapid Acidification of the Ocean during the Paleocene-Eocene Thermal Maximum, *Science*, 308, 1611–1615, 2005.
- Zachos, J. C., Schouten, S., Bohaty, S., Quattlebaum, T., Sluijs, A., Brinkhuis, H., Gibbs, S., and Bralower, T. J.: Extreme warming of mid-latitude coastal ocean during the Paleocene-Eocene Thermal Maximum: Inferences from TEX<sub>86</sub> and Isotope Data, *Geology*, 34, 737–740, 2006.
- Zachos, J. C., Bohaty, S. M., John, C. M., McCarren, H., Kelly, D. C., and Nielsen, T.: The Palaeocene-Eocene carbon isotope excursion: constraints from individual shell planktonic foraminifer records, *Philosophical Transactions of the Royal Society A*, 365, 1829–1842, 2007.
- Zeebe, R. E. and Zachos, J. C.: Reversed deep-sea carbonate ion basin gradient during the Paleocene-Eocene thermal maximum, *Paleoceanography*, 22, doi:10.1029/2006PA001395, 2007.
- Zeebe, R. E., Zachos, J. C., and Dickens, G. R.: Carbon dioxide forcing alone insufficient to explain Palaeocene-Eocene Thermal Maximum warming, *Nature Geoscience*, 2, 576–580, 2009.